

Band-to-Band Tunneling in Carbon Nanotube Field-Effect Transistors

J. Appenzeller,¹ Y.-M. Lin,¹ J. Knoch,² and Ph. Avouris¹

¹IBM T.J. Watson Research Center, Yorktown Heights, New York 10598, USA

²Institut für Schichten und Grenzflächen, Forschungszentrum Jülich, D-52425 Jülich, Germany

(Received 25 June 2004; published 4 November 2004)

A detailed study on the mechanism of band-to-band tunneling in carbon nanotube field-effect transistors (CNFETs) is presented. Through a dual-gated CNFET structure tunneling currents from the valence into the conduction band and vice versa can be enabled or disabled by changing the gate potential. Different from a conventional device where the Fermi distribution ultimately limits the gate voltage range for switching the device on or off, current flow is controlled here by the valence and conduction band edges in a bandpass-filter-like arrangement. We discuss how the structure of the nanotube is the key enabler of this particular one-dimensional tunneling effect.

DOI: 10.1103/PhysRevLett.93.196805

PACS numbers: 73.63.Fg, 73.23.-b, 73.61.Wp

Carbon nanotube field-effect transistors (CNFETs) have been the topic of studies in the past few years, in particular, because of their excellent electrical properties. So far, two types of transistor operation have been obtained. Conventional metal oxide semiconductor field-effect transistor (MOSFET)-like behavior has been reported for larger diameter carbon nanotubes. Here, the rather small energy gap allows injection from the metal contact into the valence band of the nanotube without a substantial Schottky barrier involved [1]. Consequently, for these devices it is mainly the potential barrier between the contacts that controls the current. The other type of nanotube transistor fabricated mainly from larger gap carbon nanotubes is the so-called Schottky barrier (SB)-CNFET [2,3]. In this class of devices the gate field impacts the thickness of the Schottky barriers at the metal-nanotube interface and makes them more or less transparent for tunneling from the source or drain electrodes into the nanotube channel. While tunneling in itself is a well-known effect, it has been found that the electrostatic conditions in an object as small as the nanotube result in drastically different band bending conditions than in conventional three-dimensional (3D) semiconductors [4]. In particular, very small depletion lengths L_D can be obtained in a CNFET with thin gate dielectrics, and tunneling currents can become substantial [5].

In this Letter, we present experimental and simulation results on the band-to-band (BTB) tunneling in SB-CNFETs, i.e., gate induced tunneling from the conduction into the valence band of a semiconducting carbon nanotube and vice versa. We discuss a device concept that explicitly makes use of the particular tunneling properties of nanotube devices enabling a switching between the transistor on and off states that is much more abrupt than what can be obtained with conventional field-effect transistors (FETs). Temperature dependent measurements are used to confirm that the tunneling process proposed is indeed responsible for the electrical characteristics obtained.

In order to study BTB tunneling in CNFETs, fields along the length of a tube have to be created that are strong enough to shift the conduction and valence band relative to each other by at least the gap energy of the semiconductor. Previous works have used local chemical doping of the nanotube to accomplish this task [6,7]. However, since gating in those devices occurs over the entire tube length, the tunneling conditions cannot be altered by the gate once dopants are introduced. In order to overcome this obstacle and to explore the possibility of using CNFETs as *tunable*, three-terminal tunneling devices, we have designed devices that control the electrostatics in the nanotube channel by means of two independent gates, both of which are located underneath the carbon nanotube. A top view scanning electron microscope (SEM) image as well as a schematic cross section view of our device layout are depicted in Fig. 1. Electron beam lithography is used to define all critical structures. First, a 20 nm thick and approximately $L_{Al} = 200$ nm wide aluminum (Al) layer is deposited on a highly *p*-doped silicon wafer covered with a $t_{ox-Si} = 10$ nm thick SiO_2 film. After oxidation of the Al in a water-rich environment at around 160 °C for 1 1/2 h, single wall carbon nanotubes produced by laser ablation are spun from solution onto the substrate. The Al_2O_3 thickness as determined from ellipsometry is around $t_{ox-Al} = 4$ nm [8]. Finally, source and drain electrodes from titanium (Ti) are defined with a small spacing of around $L_{Si} = 200$ nm between both contact areas and the Al gate. In this way the silicon backgate (Si gate) can control the electrostatics in the areas close to the source and drain, while the Al gate impacts the bulk part (middle portion) of the CNFET. Since the aluminum layer also screens the field from the Si gate, the potential of the nanotube in the middle is exclusively determined by the Al gate giving rise to ideal switching behavior.

Our devices operate as follows: If the gate voltage at the silicon back gate (V_{gs-Si}) is kept at a constant negative value and the voltage at the aluminum gate (V_{gs-Al}) is

swept from negative to positive, currents can flow through the device for either very high positive or negative V_{gs-Al} . The situation is illustrated in the two lower graphs of Fig. 2. In case (a), a hole current flows from the source to the drain due to thin enough barriers at the contacts and no apparent barrier in the middle region of the CNFET. This is the conventional MOSFET operation principle characterized by a thermal emission current I_{d-th} over a V_{gs-Al} -dependent barrier in the middle of the transistor. We will refer to $I_{d-th}(V_{gs-Al})$ in the following as the p -type branch. In case (b), on the other hand, BTB tunneling is enabled for high enough positive V_{gs-Al} in the transition regions between the two gates. The current through the device becomes a pure tunneling current (I_{d-tun}). What makes the case special for a CNFET is the width of the transition region ($\sim L_D$) marked by the dashed lines in case (b). Because of the small diameter (t_{ch}) of a carbon nanotube, tunneling barriers as thin as a couple of nanometers can be obtained if thin gate insulators (t_{ox}) are used [5]. This is the case since, different from a conventional semiconductor, L_D in case of a carbon nanotube is a function of t_{ch} and t_{ox} rather than only doping. The combination of small t_{ch} and t_{ox} not only allows one to obtain substantial tunneling currents, but also, and more importantly, it is the key ingredient for a very abrupt change of the device current I_d as a function of the gate voltage [9].

$I_d(V_{gs-Al})$ as measured for one of our CNFETs is shown in the main panel of Fig. 2. One can easily identify the aforementioned two current regions: the p -type

branch (a) and the BTB tunneling branch (b). Most importantly, the experiment clearly supports the statement above about the switching in CNFETs, i.e., that the inverse subthreshold slope $S = (d \log I_d / dV_{gs})^{-1}$ can be smaller than $k_B T \ln 10 / q \approx 60$ mV/dec at room temperature, the minimum value attainable for any conventional operating MOSFET [10] (k_B , T , and q are the Boltzmann constant, the temperature, and the charge, respectively). We find an S value of ~ 65 mV/dec for the p -type branch of the CNFET close to the ideal value for thermal emission [11] and ~ 40 mV/dec for the BTB tunneling branch under the measurement conditions indicated in the caption of Fig. 2. This is to the best of our knowledge the first experimental observation of a transistor operation with a slope better than 60 mV/dec due to controlled tunneling in any material system [12]. The reason that $(d \log I_{d-tun} / dV_{gs})^{-1}$ can become smaller than around 60 mV/dec at room temperature is the bandpass-filter-like operation of the BTB tunneling device. A tunneling current can flow only once the conduction band in the aluminum gated region bends below the valence band in the source area that is controlled by the silicon back gate. The two critical aspects that enable the dramatic change of I_{d-tun} are that (i) the two band edges cut off portions of the high energetic tail of the electron/

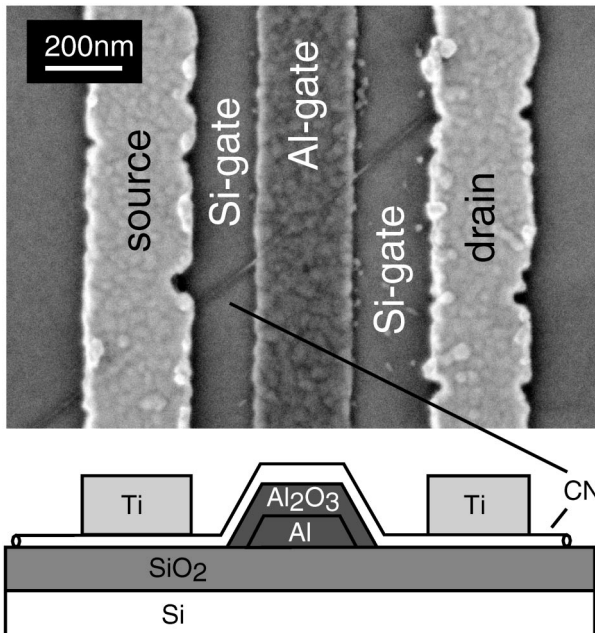


FIG. 1. SEM of a band-to-band tunneling device. The schematic in the bottom portion of the figure shows the vertical arrangement of gates, contacts, and the nanotube.

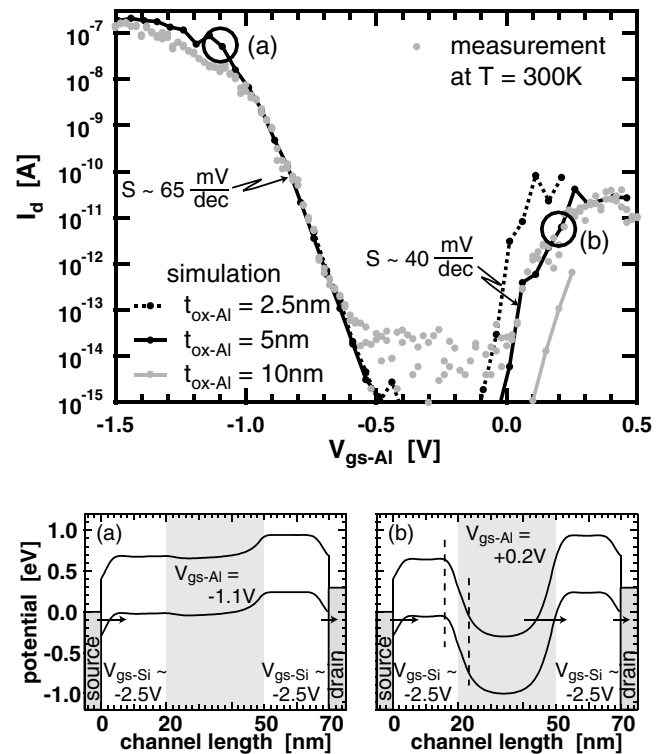


FIG. 2. $I_d(V_{gs-Al})$ for a drain voltage of $V_{ds} = -0.5V$ and $V_{gs-Si} = -3V$. Simulated electrical characteristics are for three different t_{ox-Al} and $t_{ox-Si} = 10$ nm with corresponding values for the dielectric constants of 5 and 4, respectively.

hole Fermi distribution and (ii) the tunneling distance decreases rapidly for thin enough $t_{\text{ox-Al}}$ when $V_{\text{gs-Al}}$ is changed due to the one-dimensional nature of the carbon nanotube.

Next, we present simulated characteristics of a CNFET under the distinct field conditions explored here. Simulations were performed by considering a CNFET consisting of a nanotube in contact with two semi-infinite source or drain metallic contacts. The charge in and current through the CNFET are calculated self-consistently using the nonequilibrium Green's function formalism [13] together with a modified 1D Poisson equation due to Young [14] that accounts for the impact of gate oxide thickness and tube diameter on the electrostatics. A quadratic dispersion relation is assumed in the conduction and valence band; the complex band structure in the semiconductor gap is taken into account by an energy dependent effective mass [15].

The main panel of Fig. 2 also contains the results of three simulation runs. Parameters used are indicated in the figure and its caption. In particular, we assume an energy gap of $E_{\text{gap}} = 0.7$ eV. To keep computational time at a minimum, we have identified a channel length of $L_{\text{Al}} = 30$ nm and $L_{\text{Si}} = 20$ nm to be sufficient to describe the situation in a “long-channel” CNFET, a device for which increasing L_{Al} or L_{Si} does not impact I_d . The agreement between the curve for $t_{\text{ox-Al}} = 5$ nm and the experimental data is excellent over the entire gate voltage range. (Note in this context that the resolution limit in our measurement is around 10 fA.) This not only highlights the quality of our model but also it is convincing evidence for the above interpretation of BTB tunneling in CNFETs. Comparing the simulations for different $t_{\text{ox-Al}}$ also reveals the previously discussed trend of smaller values of S in the BTB tunneling branch for thinner gate oxides.

To further evaluate our interpretation and to eliminate reasons other than BTB tunneling for the occurrence of the right branch in Fig. 2, we have performed two more supporting experiments. First, we investigated the temperature dependence of the device characteristics. As has been pointed out before in the context of Schottky barriers [3,5], the temperature dependence of S is a useful measure to distinguish between thermal emission contributions and those mediated by tunneling. Here we make use of the $S(T)$ dependence to check whether tunneling is indeed responsible for the change of current in the BTB tunneling branch. Figure 3 shows the result of this experiment. For negative Al-gate voltages in the p -type branch, $S = (d \log I_{d-\text{th}} / dV_{\text{gs-Al}})^{-1}$ becomes smaller with decreasing T . The change of S follows, in principle, the expected trend for thermal emission as apparent from the inset. Experimental data are marked as gray symbols with error bars, while the simulation results are shown as a solid gray line with markers. On the other hand, the

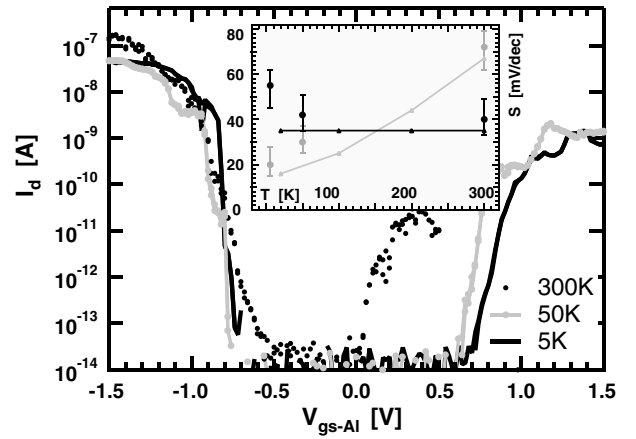


FIG. 3. Subthreshold characteristics for a band-to-band tunneling device at three different temperatures. The inset shows the extracted S values for the p -type branch at $V_{\text{gs-Al}} < 0$ as gray symbols with error bars and those extracted from the BTB tunneling branch at $V_{\text{gs-Al}} > 0$ as black symbols with error bars. Also included are simulation results as solid lines with markers.

slope of the BTB tunneling branch $S = (d \log I_{d-\text{tun}} / dV_{\text{gs-Al}})^{-1}$ remains rather unchanged or even increases slightly for the lowest temperatures. This dependence that is expected for a tunneling-dominated transport across the nanotube channel is also included in the inset of Fig. 3 (see black symbols and lines). Clearly, both trends are different enough to distinguish between them. In particular, both the experimental data and the simulation show a “crossover” at a temperature between 100 and 200 K, meaning that S is larger for the thermal emission contribution than for BTB tunneling at room temperature, while the situation is reversed at low T . This particular behavior cannot be explained within a model other than the BTB tunneling interpretation proposed here.

It is worth mentioning that transistors in a highly integrated circuit typically operate at temperatures well above 300 K and that under these conditions S values substantially larger than 60 mV/dec are obtained for currents controlled by thermal emission. The advantage of using tunnel currents instead in this regime is obvious from the inset of Fig. 3.

Second, we have explored how far the electrical characteristics of our tunneling devices change as a function of the silicon backgate voltage $V_{\text{gs-Si}}$. Figure 4 shows a typical example of such a measurement [16]. As before, we are scanning the Al-gate voltage and keep the Si-gate voltage fixed. This is done for $V_{\text{gs-Si}}$ values ranging from -1.5 V to $+1.0$ V. We will focus our discussion on the device current for positive $V_{\text{gs-Al}} \approx +1.0$ V. At highly negative Si-gate voltages (case ①), we observe currents of around $\sim 10^{-11}$ A. By increasing $V_{\text{gs-Si}}$ the current drops down by more than 2 orders of magnitude (see

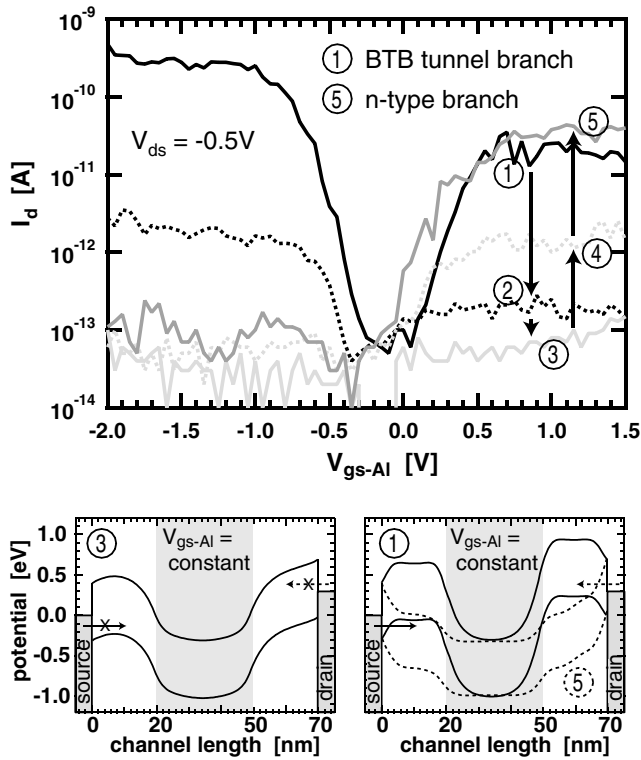


FIG. 4. Main panel: Electrical characteristics of a BTB CNFET for various silicon backgate voltages. Cases ① to ⑤ are obtained for $V_{gs-Si} = -1.5V, -1.0V, -0.5V, 0V,$ and $+1.0V$ respectively. Lower panels depict the band bending situation for cases ①, ③, and ⑤ at positive V_{gs-Al} qualitatively.

cases ② and ③). Further increasing the Si-gate voltage to more positive values increases the current again (cases ④ and ⑤). It is this strongly nonmonotonic behavior that is the key finding in this experiment. The dependence of I_d on V_{gs-Si} can be easily understood as the transition from the BTB tunneling regime to a pure n -type electron current, as we will discuss now. The lower two panels of Fig. 4 qualitatively illustrate the evolution. While in case ① a BTB tunneling current is enabled (black arrow), and in case ⑤ an electron current can be injected from the drain side (dashed arrow), both of these current paths are forbidden in case ③. The reason is that for an intermediate Si-gate voltage range current flow gets blocked in the source and drain regions by the nanotube band gap. The device turns on only if the contact barriers are either thin enough for hole *or* electron injection, which occurs only at sufficiently negative *or* positive V_{gs-Si} . As stated before, this particular nonmonotonic behavior cannot be easily explained within any other model and is final evidence for band-to-band tunneling in CNFETs under the right gate and drain voltage conditions.

In conclusion, we have shown that band-to-band tunneling can be substantial in CNFETs at room tempera-

ture. In particular, we have found that the observed very abrupt switching in our devices as apparent from the extremely small inverse subthreshold slope in Fig. 2 is a result of a tunable tunneling current in a CNFET. Our results elucidate the nature of band-to-band tunneling in low-dimensional structures and the substantial differences between nanoscale and conventional semiconductors.

-
- [1] A. Javey, J. Guo, Q. Wang, M. Lundstrom, and H. Dai, *Nature (London)* **424**, 654 (2003).
 - [2] S. Heinze, J. Tersoff, R. Martel, V. Derycke, J. Appenzeller, and Ph. Avouris, *Phys. Rev. Lett.* **89**, 106801 (2002).
 - [3] J. Appenzeller, J. Knoch, V. Derycke, R. Martel, S. Wind, and Ph. Avouris, *Phys. Rev. Lett.* **89**, 126801 (2002).
 - [4] F. Leonard and J. Tersoff, *Phys. Rev. Lett.* **84**, 4693 (2000).
 - [5] J. Appenzeller, M. Radosavljević, J. Knoch, and Ph. Avouris, *Phys. Rev. Lett.* **92**, 048301 (2004).
 - [6] Ch. Zhou, J. Kong, E. Yenilmez, and H. Dai, *Science* **290**, 1552 (2000).
 - [7] J. Kong, J. Cao, and H. Dai, *Appl. Phys. Lett.* **80**, 73 (2002).
 - [8] A completely Al/Al₂O₃ backgated CNFET was first presented by Bachtold *et al.* [*Science* **294**, 1317 (2001)].
 - [9] Different from the device concept discussed by Leonard and Tersoff [*Phys. Rev. Lett.* **88**, 258302 (2002)] our approach does not rely on the resonant tunneling through zero-dimensional states in a quantum-dot-like nanotube structure.
 - [10] S. M. Sze, *Physics of Semiconductor Devices* (Wiley, New York, 1981).
 - [11] Y.M. Lin, J. Appenzeller, and Ph. Avouris, in *Proceedings of the 62th Device Research Conference, 2004* (IEEE, New York, 2004), p. 133.
 - [12] Javey *et al.* [*Nano Lett.* **4**, 447 (2004).] recently reported transport measurements on devices that, at first glance, resemble those used here. However, these devices are around 5 times longer than ours, making them operate in the diffusive transport regime, and are based on rather small band gap tubes, preventing the observation of extremely small device off currents as necessary for the experiments presented here.
 - [13] S. Datta, *Electronic Transport in Mesoscopic Systems* (Cambridge University Press, Cambridge, 1998).
 - [14] K. Young, *IEEE Trans. Electron Devices* **36**, 399 (1992).
 - [15] H. Flietner, *Phys. Status Solidi B* **54**, 201 (1972).
 - [16] Not all devices showed electrical characteristics with S values as small as those shown in Figs. 2 and 3. We find that in these cases the slope of both the p -type branch and the BTB tunneling branch are shallower than anticipated. This effect is likely a result of parasitic capacitance contributions from the unpassivated SiO₂ and/or Al₂O₃ surface.